Molecular Therapy
Methods & Clinical Development
Original Article

Genome-wide Specificity of Highly Efficient TALENs and CRISPR/Cas9 for T Cell Receptor Modification

Friederike Knipping,[1] Mark J. Osborn,[2,3,4,5] Karl Petri,[1] Jakub Tolar,[2,3,4,5] Hanno Glimm,[1] Christof von Kalle,[1] Manfred Schmidt,[1] and Richard Gabriel[1]

[1]Department of Translational Oncology, National Center for Tumor Diseases and German Cancer Research Center, 69120 Heidelberg, Germany; [2]Division of Blood and Marrow Transplantation, Department of Pediatrics, University of Minnesota, Minneapolis, MN 55455, USA; [3]Center for Genome Engineering, University of Minnesota, Minneapolis, MN 55455, USA; [4]Stem Cell Institute, University of Minnesota, Minneapolis, MN 55455, USA; [5]Asan-Minnesota Institute for Innovating Transplantation, Seoul 05505, Republic of Korea

In T cells with transgenic high-avidity T cell receptors (TCRs), endogenous and transferred TCR chains compete for surface expression and may pair inappropriately, potentially causing autoimmunity. To knock out endogenous TCR expression, we assembled 12 transcription activator-like effector nucleases (TALENs) and five guide RNAs (gRNAs) from the clustered regularly interspaced short palindromic repeats (CRISPR)/CRISPR-associated (Cas9) system. Using TALEN mRNA, TCR knockout was successful in up to 81% of T cells. Additionally, we were able to verify targeted gene addition of a GFP gene by homology-directed repair at the TALEN target site, using a donor suitable for replacement of the reporter transgene with therapeutic TCR chains. Remarkably, analysis of TALEN and CRISPR/Cas9 specificity using integrase-defective lentiviral vector capture revealed only one off-target site for one of the gRNAs and three off-target sites for both of the TALENs, indicating a high level of specificity. Collectively, our work shows highly efficient and specific nucleases for T cell engineering.

INTRODUCTION

The introduction of high-avidity T cell receptor (TCR) genes into mature T cells for adoptive T cell therapy is a highly effective method for enhancing TCR specificity.[1,2] However, the competition of co-expressed endogenous and transgenic TCR chains for the limited components of the CD3 complex may lead to suboptimal surface expression and impaired function of both receptors.[3] Further, mispairing of the endogenous and exogenous α and β chains may trigger host antigen recognition and autoimmunity, because the mixed TCR dimers are not subjected to thymic selection. Such a phenomenon has been observed in mouse models for TCR gene therapy, where self-reactive T cells led to lethal graft versus host disease (GvHD).[4] In another study, the introduction of TCR genes into human T cells resulted in the formation of neoreactive mispaired TCRs, some of which displayed autoreactivity.[5] A novel method for preventing this is the disruption of the endogenous TCR genes so that the transgenic TCR alone is expressed on the cell surface. Rationally designed engineered nucleases have been employed to accomplish this.[6]

The major classes of gene-editing proteins are the zinc-finger nucleases (ZFNs), meganucleases, transcription activator-like effector nucleases (TALENs), and the RNA-guided nucleases of the *Streptococcus pyogenes* (Sp) clustered regularly interspaced short palindromic repeats (CRISPR)/CRISPR-associated (Cas9) system. These reagents can be employed for gene modification by introducing targeted DNA double-strand breaks (DSBs).[7,8] DSB repair by error-prone non-homologous end joining (NHEJ) can result in gene disruption because of frameshift mutations. Homology-directed repair (HDR) stimulated by a DSB enables both correction of genomic mutations and targeted transgene integration when a homology-containing donor template is provided in *trans* (Figure 1A).

TALENs are functional dimers consisting of DNA-binding domains fused to a FokI endonuclease catalytic domain. Upon co-localization of the FokI subunits tethered to the two TALEN-monomers, a DSB is introduced at the target site (Figure 1A).[9] The chimeric guide RNA (gRNA) of the CRISPR/Cas9 system promotes Cas9-mediated DSB introduction by base-pairing between its 5′ sequence of 20 bases and a DNA target site. The full target site for SpCas9 must contain a target profile of $GN_{19}NGG$, with the terminal three bases referred to as a protospacer adjacent motif (PAM).[10,11] Designer nucleases have been reported to induce DSB not only at their target sites, but also at other genomic loci that contain sequence similarity, termed off-target sites. To examine the quantity and characteristics of these events, several studies have established in silico prediction methods,[12] in vitro cleavage site analysis,[13] systematic mismatching of various target site positions,[14] and genome-wide off-target detection.[15–20]

Studies to date designed to prevent the assembly of TCRs with unknown specificity have employed RNAi-mediated TCR knockdown and ZFN- or TALEN-mediated TCR knockout.[6,20–22] Here, we report the generation and employment of highly efficient and specific TALENs and CRIPSR/Cas9 to safely edit the human TCR locus. In order to disrupt the endogenous TCR, we generated 12 TALENs and five CRISPR/Cas9 gRNAs specific for the constant regions of

Received 11 January 2017; accepted 25 January 2017;
http://dx.doi.org/10.1016/j.omtm.2017.01.005.

Correspondence: Richard Gabriel, German Cancer Research Center, Im Neuenheimer Feld 581, 69120 Heidelberg, Germany.
E-mail: richard.gabriel@nct-heidelberg.de

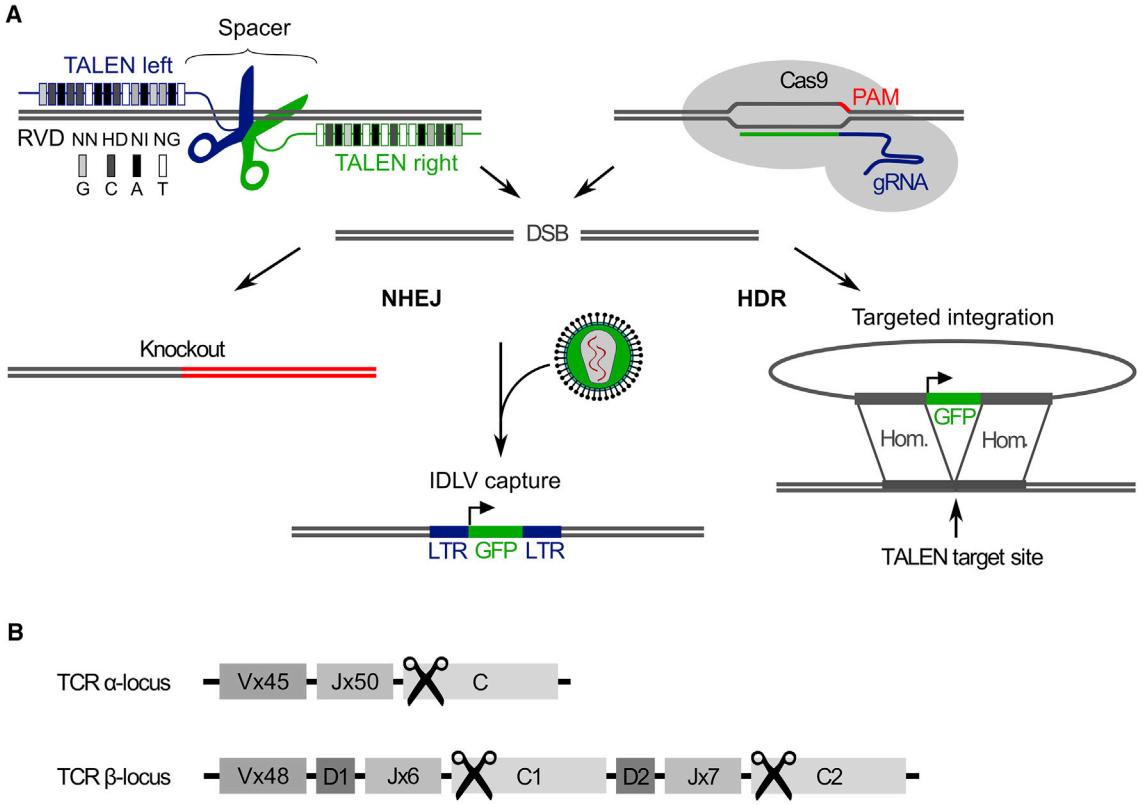

Figure 1. DSB Repair and Targeted Genome Editing of the TCR Loci Using Designer Nucleases

(A) During NHEJ-repair of TALEN- and CRISPR/Cas9-induced DSBs, frameshift mutations can result in gene knockout, or episomal IDLV can be integrated into DSBs, allowing for the permanent marking of off-target DSBs. If donor DNA is provided, HDR can lead to targeted integration of an expression cassette, i.e., therapeutic TCR chains. (B) The TCR α and β locus are composed of a number of variable (V), joining (J), constant (C), and, in the case of *TRBC*, diversity (D) gene segments (numbers of functional genes from IMGT/GENE-DB[53] version 3.1.16, December 14, 2016). The positions of TALEN and gRNA target sequences for TCR knockout in the TCR α constant region (*TRAC*) and a homologous sequence shared by both TCR β constant regions (*TRBC1/2*) are marked by scissor symbols. DSB, DNA double-strand break; gRNA, guide RNA; HDR, homology-directed repair; IDLV, integrase-defective lentiviral vector; LTR, long terminal repeat; NHEJ, non-homologous end joining; PAM, protospacer adjacent motif; RVD, repeat variable di-residue.

the TCR α and β chain genes (*TRAC* and *TRBC1/2*) (Figure 1B). To assess the specificity of the reagents, we performed an unbiased genome-wide off-target analysis by integrase-defective lentiviral vector (IDLV) capture into TALEN- and CRISPR/Cas9-mediated DSBs in cultured cells. This analysis showed near exclusivity of DSB generation at the TALEN and CRISPR/Cas9 target sites, demonstrating a high level of specificity. We furthermore show HDR-mediated, targeted integration of a GFP-expression cassette into the *TRAC* locus. The donor IDLV is designed for subsequent exchange of the GFP cassette for user-defined TCR genes, thereby representing a tool for the generation of therapeutic T cells with high-avidity TCR.

RESULTS

Design and Construction of Designer Nucleases

We designed a set of TALENs and CRISPR/Cas9 gRNAs to disrupt endogenous TCR expression. Aiming at a direct comparison of both platforms while excluding locus inherent effects, we chose partly overlapping target sites. We constructed eight TALENs to induce specific DSBs in the constant region of the TCR α chain (*TRAC*, αT2-9) and four TALENs targeting both constant regions of the TCR β chain (*TRBC1* and *TRBC2*; βT1-4) (Figures 2A and 2D; Table S1). For constructing the TALEN candidates, we used the pTAL3 scaffold (T_P) published by Cermak et al.,[9] the GoldyTALEN (T_G),[23] and the comparable CAG-T7-TALEN (Sangamo)-Destination (T_S) scaffold that possess shortened linkers between DNA-binding domain and FokI domain, as well as alternate mutations for promoting heterodimeric pairing [T_{SOH}; CAG-T7-TALEN(Sangamo)-FokI-ELD-Destination and CAG-T7-TALEN (Sangamo)-FokI-KKR-Destination] (Table S1).[24] This TALEN architecture has been reported to have a strong impact on TALEN activity as well as specificity.[25–27] Six of the TALENs with the pTAL3 scaffold shared one or both monomers with other TALENs to create TALENs separated by 12 and 15 bp spacers, respectively. Obligate heterodimeric (OH) FokI domains were used to prevent homodimeric pairing of left or right TALEN arrays, thereby minimizing the risk for off-target activity.[28] In addition, we subcloned TALEN

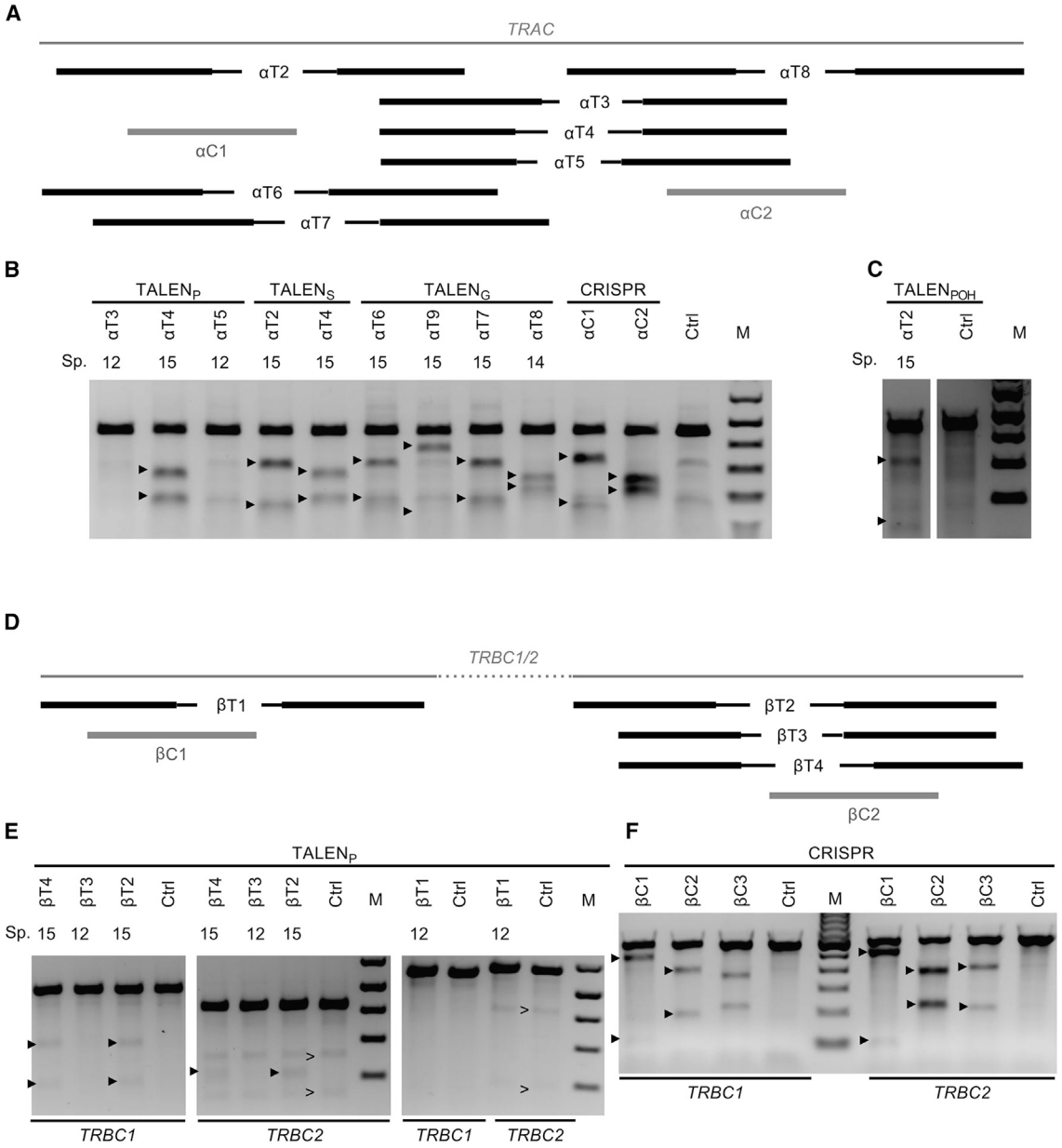

Figure 2. Evaluation of TALEN and CRISPR/Cas9 Activity

(A) Positions of TALEN and CRISPR/Cas9 gRNA binding sites at the *TRAC* target site. (B) TALEN and CRISPR/Cas9 activity in the *TRAC* locus in K562 cells. (C) Activity of obligate heterodimeric TALENs in the *TRAC* locus in 293T cells. (D) TALEN and gRNA binding sites at *TRBC1* and *TRBC2* target locus. (E) TALEN activity in the *TRBC1* and *TRBC2* locus in 293T cells. (F) CRISPR/Cas9 activity in the *TRBC1* and *TRBC2* locus in K562 cells. (B, C, E, and F) PCR amplification of the target regions in the TCR loci produces upper bands. T7EI-mediated cleavage of NHEJ-originated heteroduplex DNA results in additional cleavage bands, marked by arrowheads. A SNP in the *TRBC2* locus results in additional bands, marked by arrows (>). Ctrl, negative control; M, marker; Sp., length of spacer between TALEN binding sites in base pairs; TALEN$_G$, GoldyTALEN; TALEN$_{P(OH)}$, pTAL3 (obligate heterodimeric FokI domain); TALEN$_S$, CAG-T7-TALEN(Sangamo)-Destination.

αT4 and βT4 into the RCIscript Goldy backbone that is suitable for in vitro transcription.[27]

In parallel, we evaluated RNA-guided nucleases of the CRISPR/Cas9 system for TCR gene editing. We designed two and three different gRNAs for the constant regions of the TCR α chain (αC1 and αC2) and the TCR β chain (βC1-3), respectively, that overlapped with the corresponding TALEN target sites (Figures 2A and 2D; Table S1). Using in silico predictive software, we chose sites containing high sequence fidelity for the Cas9 nuclease. In addition, to ascertain

Table 1. Indel Frequency at TALEN and CRISPR/Cas9 Target Sites

Nuclease	% Indel
TRAC Locus	
$\alpha T2_S$	42.3
$\alpha T2_{POH}$	3.5^T
$\alpha T4_P$	19.4^T/26.2
$\alpha T4_S$	27.0
$\alpha T4_m$	18.4
$\alpha T6_G$	16.7
$\alpha T7_G$	33.4
$\alpha T8_G$	21.4
$\alpha T9_G$	41.9
αC1	67.3
αC2	76.5
TRBC1 Locus	
$\beta T2_P$	4.2^T
$\beta T3_P$	0.0^T
$\beta T4_P$	3.0^T/8.6
$\beta T4_{POH}$	0.1^T
$\beta T4_S$	4.1
$\beta T4_m$	9.5
βC2	52.3
TRBC2 Locus	
$\beta T2_P$	4.5^T
$\beta T3_P$	0.0^T
$\beta T4_P$	1.9^T/16.7
$\beta T4_{POH}$	1.3^T
$\beta T4_S$	10.3
$\beta T4_m$	20.5
βC1	59.5
βC3	24.7

% Indel denotes the frequency of sequences with insertions or deletions at the respective nuclease target sites analyzed by deep sequencing. Values with superscript T were obtained in 293T cells; all other results were generated in K562 cells. C, CRISPR/Cas9; T_G, GoldyTALEN; T_m, TALEN delivered as mRNA; $T_{P(OH)}$, pTAL3 (obligate heterodimeric FokI domain); T_S, CAG-T7-TALEN(Sangamo)-Destination.

the relative accuracy of in silico modeling, we also included one gRNA (βC3) with a low "quality score" intended as a control for off-target analysis. For CRISPR/Cas9 generation we used the pX330 expression plasmid.[10]

TALEN and CRISPR/Cas9 Activity at Their Target Sites

After delivery of TALEN or Cas9/gRNA-expressing plasmids to K562 cells by nucleofection or to 293T cells using *polyethylenimine* (PEI) transfection, TALEN and CRISPR/Cas9 activities were examined using the T7 endonuclease I (T7EI) assay. All TALENs with monomers separated by a 14 bp or 15 bp spacer induced specific DSBs at their target sites, whereas TALENs separated by 12 bp spacers failed to do so (Figure 2; Figure S1). In contrast to previous reports, obligate heterodimeric TALENs were less efficient than wild-type FokI domains (Table 1; Figure S1).[29,30] When expressed from the T_{SOH} vectors, the heterodimeric TALENs did not show locus-specific activity at the resolution of the T7EI assay (data not shown).

To quantify the nuclease cleavage activities, we further analyzed PCR-amplified nuclease target sites by deep sequencing. TALEN and CRISPR/Cas9 target locus activity in K562 cells resulted in up to 42.3% and 76.5% of sequences with insertions or deletions (indels), respectively (Table 1). Although the α chain TALENs delivered as plasmid showed superior efficiency compared with the β chain TALENs, nucleofection with TALEN mRNA increased the cleavage efficiency of βT4, but not of αT4. The deep sequencing results of all analyzed *TRBC* samples showed higher editing rates in the C2 region than in the C1 region (Figures 2 and 3; Table 1). Using an alternative C1 forward primer that binds with high target specificity upstream of the C1/C2 homologous region, we showed that in a proportion of the cells, simultaneous cleavage at the respective target sites in C1 and C2 resulted in the deletion of the complete sequence between both target sites (Figure S2).

Knockout of Endogenous TCR Expression in T Lymphocytes

After confirming TALEN and CRISPR/Cas9 activity in K562 cells, we evaluated their efficacy for TCR knockout in primary T cells. Using electroporation-based gene transfer of TALEN-expressing plasmid DNA ($\alpha T4_P$), we achieved up to 12.2% TCR knockout in primary T cells, determined by loss of CD3 surface expression (Figure S3). Flow cytometric analysis of T cells electroporated with CRISPR/Cas9-expressing plasmids revealed a TCR knockout efficiency rate of 19.9% (16.6% ± 1.7%, mean ± SD) for *TRAC*-specific αC2 and 16.6% (14.2% ± 2.1%) for *TRBC1/C2*-specific βC2 (Figure 3A). The nuclease activity was additionally confirmed by T7EI assay and deep sequencing analysis of PCR products. Nineteen percent of sequences of αC2-treated cells, 6.3% of *TRBC1*, and 12.5% of *TRBC2* sequences of βC2-treated cells contained indels (Figure 3B).

Because previous reports have demonstrated enhanced disruption rates following mRNA delivery of nucleases, we delivered TALEN αT4 and βT4 mRNA ($\alpha T4_m$ and $\beta T4_m$) to primary T cells by electroporation. We observed an increase in cell viability of transfected T cells, as well as a marked increase in TCR knockout efficiency rate of 78.8% (75.1% ± 2.5%) for $\alpha T4_m$ and 81.2% (76.6% ± 3.8%) for $\beta T4_m$ on day 6 after electroporation (Figure 3C; Figure S4).[21,31] This result was confirmed by T7EI assay and deep sequencing of the PCR products showing that 79.5% of the *TRAC* sequences and 52.1% and 71.4% of the *TRBC1* and *TRBC2* sequences, respectively, had nuclease-generated indels (Figure 3D). Modified T cells were able to be kept in culture for 20 days with high viability and stable TCR disruption rates as determined by flow cytometric analysis (Figure S5). The higher knockout efficiencies in T cells also resulted in higher deletion rates between the *TRBC1* and *TRBC2* regions than in K562 cells (Figure S2).

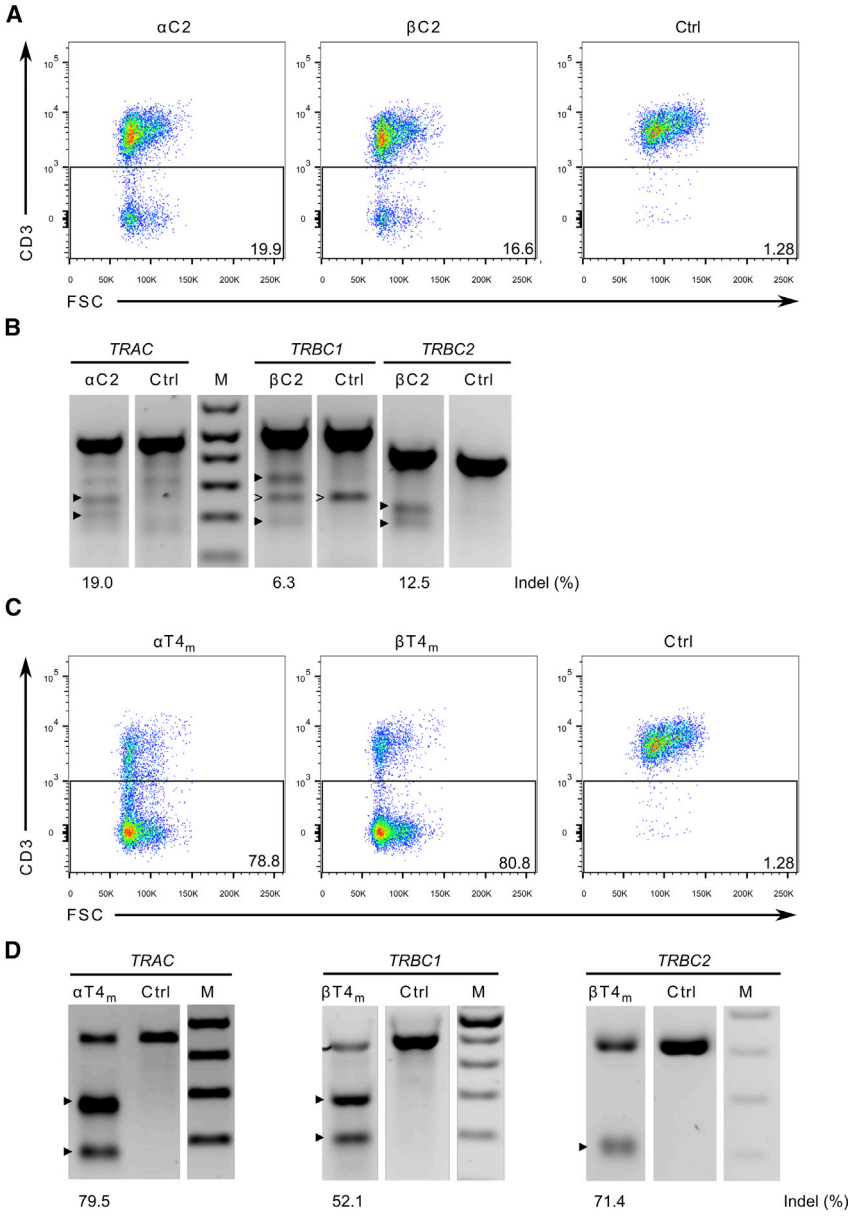

Figure 3. Analysis of CRISPR/Cas9 and TALEN-Mediated TCR Knockout in Primary T Cells

(A) Percentage of TCR knockout, evaluated by flow cytometric analysis of cell surface CD3 expression, in T cells 6 days after electroporation with αC2 or βC2. Shown are representative flow cytometry plots from four independent experiments with duplicates in T cells from three different donors. (B) Confirmation of CRISPR/Cas9 activity in T cells by T7EI assay and deep sequencing. (C) Percentage of TCR knockout, quantified by FACS, in T cells 6 days after electroporation with $\alpha T4_m$ or $\beta T4_m$. Shown are representative flow cytometry analyses of six independent experiments, with duplicates, in T cells from five different donors. (D) TALEN activity at target sites validated by T7EI assay and deep sequencing after electroporation of primary T cells with $\alpha T4_m$ or $\beta T4_m$. (B and D) Upper bands derived from wild-type PCR products and lower T7EI cleavage products are marked by arrowheads. A SNP in the *TRBC1* locus results in an additional band, marked by arrows (>). The frequency of indels was analyzed by deep sequencing of PCR products. Ctrl, untreated T cells as negative control; FSC, forward scatter; M, marker; n.d., not determined.

TRAC and *TRBC* TALENs and CRISPR/Cas9 Are Specific for Their Target Sites

Off-target activity has implications for the translational application of programmed nucleases, and each class has previously shown off-target activity.[14,16–20] To analyze the nuclease specificity for these clinically relevant loci, we transduced K562 cells with an IDLV cargo that can be captured at genomic sites where DSBs occur.[15,17,20] The transduced cells were subsequently transfected with CRISPR/Cas9 αC2 and βC1-3 plasmids and the three scaffold variants of TALEN αT4 and βT4, including mRNA. IDLV-marked DSBs were subsequently identified using linear amplification-mediated (LAM)-PCR, non-restrictive (nr) LAM-PCR, and deep sequencing.[32–35] Maximally, 3,268 IDLV integration sites were found in cells treated with or without nucleases. When two or more of these events are mapped within less than 100 nt or in more than one LAM-PCR sample replicate, they are defined as clustered integrations sites (CLISs) and are evidence of on- or off-target activity. Low-frequency off-target sites can manifest as single integration sites rather than CLISs. To validate true off-target sites, we used the sequence pattern match tool "scan-for-matches."[36] For this, regions upstream and downstream of all integration sites were scanned for potential binding sites with a maximum distance of 10 bp between integration site and predicted cleavage position and up to six or eight mismatches for gRNA or TALENs, respectively.[36] Identified on- and off-target sites were examined for NHEJ-derived indel formation by targeted deep sequencing and the CRISPResso tool[37] in order to validate the LAM-PCR data.

CLISs were observed proximal to the respective target site in all nuclease-treated samples, but not in the IDLV-only control (Table S2). In total, we detected six off-target sites for the analyzed TALEN candidates (Figure 4; Table S3). Four of these (αT4 OT3, βT4 OT1-3) were detected only in samples treated with TALEN mRNA (Tables S2 and S3). One off-target site (βT4 OT2) was indicated only by a single IDLV integration site that was located in the spacer region of a potential TALEN binding site with seven mismatches to the target site. Five off-target sites were detected in gene-coding regions and one in an

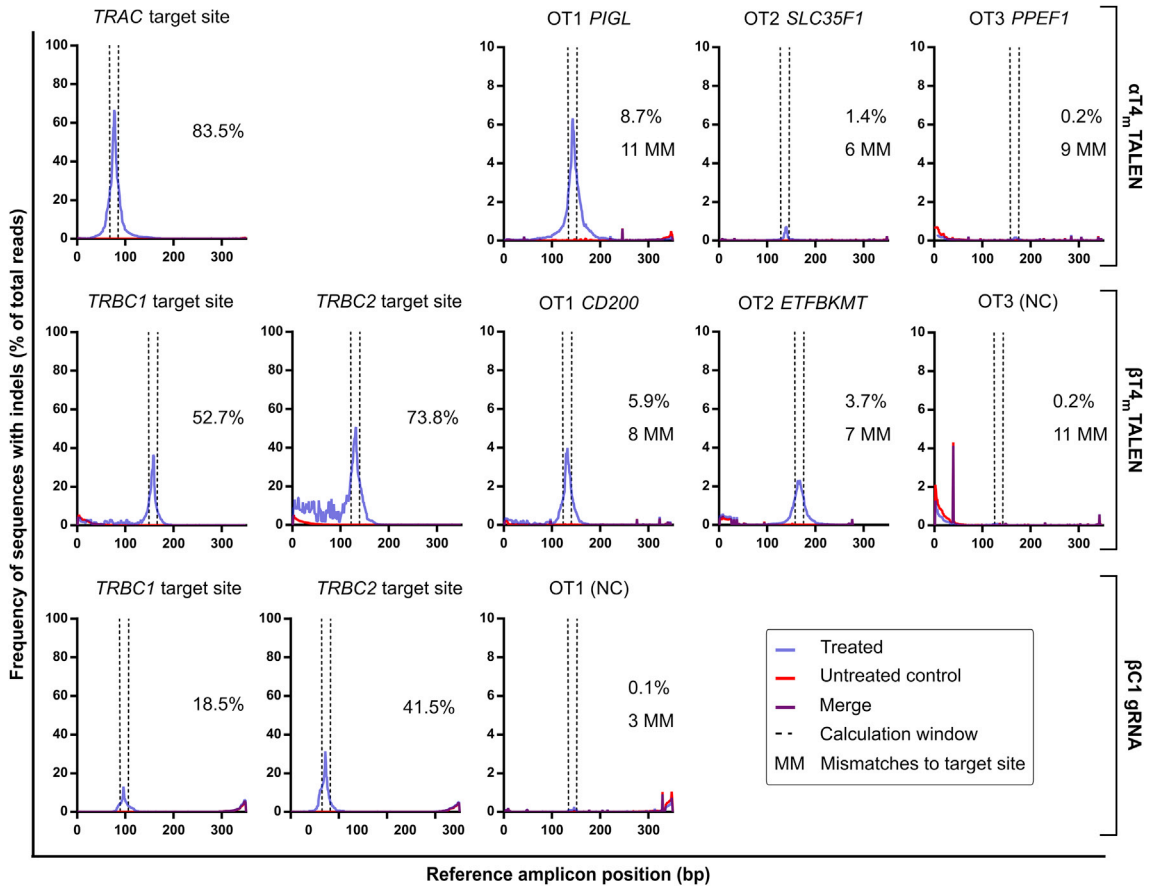

Figure 4. Quantification of NHEJ at TALEN and CRISPR/Cas9 On- and Off-Target Sites, Analyzed by Deep Sequencing and the CRISPResso Tool[37]

Percentage of sequences showing indels (combined insertions and deletions) at each position of the respective on- and off-target site amplicon in $\alpha T4_m$- and $\beta T4_m$-treated primary T cells and βC1-treated K562 cells. Only indels overlapping the specified window of 20 bp that is centered on the respective predicted cleavage site are included in the quantification indicated in each graph. MM, number of mismatches to the respective target site; NC, non-coding.

intergenic region. All off-target sites except αT4 OT3 were cleaved by a homodimer of the respective left TALEN binding domain (Table S3). Deep sequencing confirmed cleavage at all target sites with mutation frequencies of up to 16.9% (*TRAC*), 11.3% (*TRBC1*), and 17.9% (*TRBC2*). Four of the off-target sites were confirmed by deep sequencing in K562 cells with mutation frequencies of 0.1% to 0.6% (Table S4). Of the CRISPR/Cas9 candidates, only one (βC1) showed an off-target CLIS, localized in an intergenic region (Figure 4). In contrast, gRNA βC3 that was included as control with a low "quality score" showed 24 CLISs at off-target sites (Tables S2 and S5). In addition, we chose two web-based tools in order to compare their predicted with our experimentally determined off-target sites. Both the CRISPR Design tool[38] that was used for designing the TCR β chain CRISPR/Cas9 gRNA and the COSMID tool[39] predicted 7 of the 24 βC3 off-target sites identified in this study when allowing the highest possible number of mismatches (CRIPSR Design: four mismatches, COSMID: three mismatches). The COSMID tool predicted all identified off-target sites when one insertion and one deletion were allowed in addition to two mismatches. However, the total number of predicted off-target sites, in this case, was 1,197 at 823 genomic sites. Only the COSMID tool predicted the single off-target site for βC1 (Table S5).

The off-target analyses were performed in K562 because of the low proliferation rates of T cells that lack CD3 surface expression leading to insufficient dilution of episomal IDLV and amplification of predominantly non-integrated IDLV by LAM-PCR. Therefore, the off-target sites that were detected in K562 cells were validated in primary T cells by deep sequencing. The target site disruption frequency in T cells was 83.5% for *TRAC*, 52.7% for *TRBC1*, and 73.8% for *TRBC2*. Similar to the on-target editing efficiencies, the frequency of off-target sites was more prevalent in T cells than K562 (Figure 4; Table S4).

Targeted Gene Addition through HDR

Having demonstrated successful TCR knockout, the capability of αT4 to stimulate efficient targeted gene addition by HDR was evaluated. For gene addition to the *TRAC* locus, we designed and

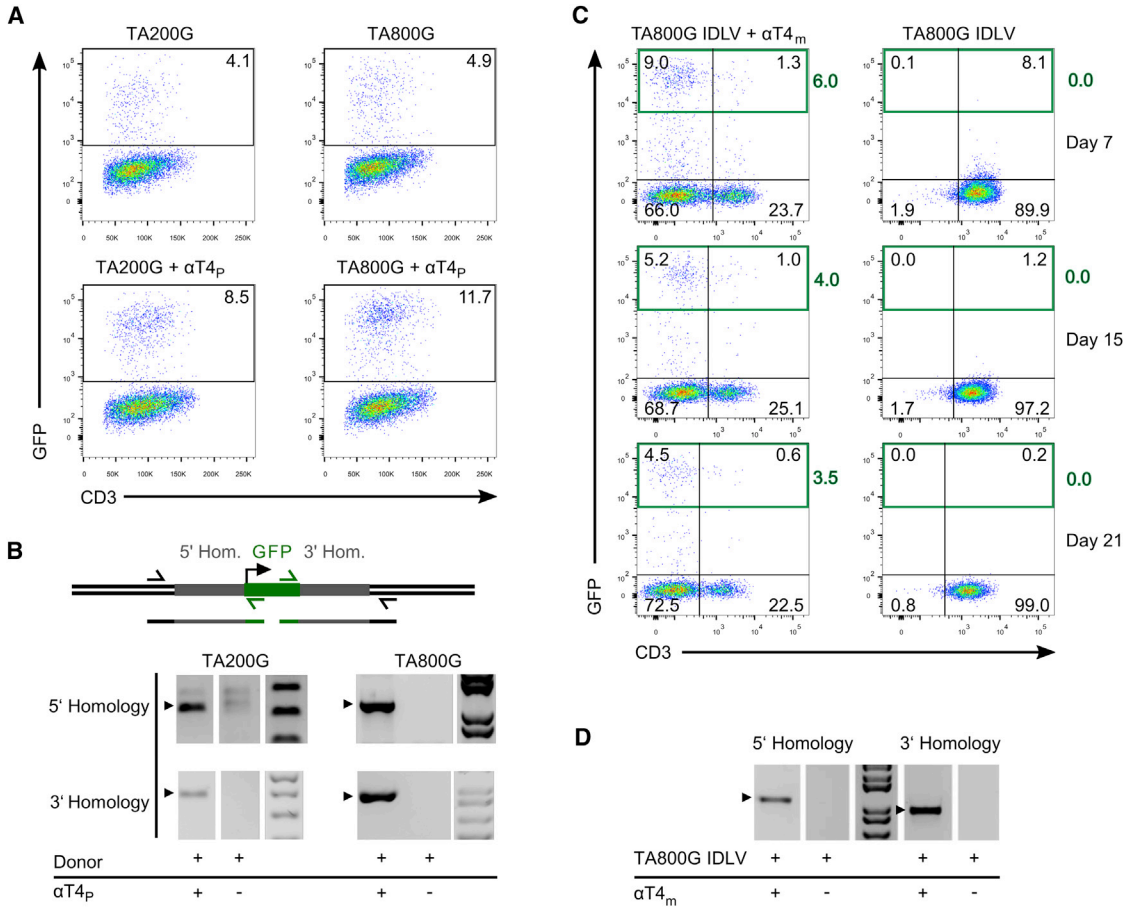

Figure 5. TALEN-Induced, HDR-Mediated, GFP Integration into the *TRAC* Locus in K562 Cells and Primary T Cells

(A) Percentage of GFP-expressing K562 cells 14 days after nucleofection with GFP-encoding donor plasmid TA200G or TA800G without (upper panel) or together with TALEN αT4$_P$ or βT4$_P$ (lower panel). Representative FACS analyses of two independent experiments are shown. (B) Validation of targeted integration into the *TRAC* locus by bidirectional PCR with primers binding in the GFP expression cassette or outside of the 5′ or 3′ homology arms, respectively. (C) Flow cytometric analysis of TCR knockout, determined by CD3 surface expression, and GFP expression of primary T cells 7, 15, and 21 days after transduction with TA800G-IDLV only (right panels) or additional electroporation with αT4$_m$ on day 1 (left panels). Shown are representative FACS analyses of three independent experiments in T cells from separate donors. (D) Validation of targeted integration into the *TRAC* locus by bidirectional PCR with primers binding in the GFP expression cassette or outside of the 5′ or 3′ homology arm, respectively (see scheme in B). PCR products are marked by arrowheads. Hom., homology region.

constructed two different donor templates containing a GFP expression cassette flanked by 200 bp (TA200G) or 800 bp (TA800G) sequences homologous to the αT4 target site. The design strategy allows for the use of the GFP reporter gene for detection and quantification, and is constructed such that it can be replaced by functional TCR sequences. After cultivation for 2 weeks, the background expression of GFP in cells not treated with TALENs was 3.8% ± 1.6% (TA200G) and 3.9% ± 1.9% (TA800G) (mean ± SD). In contrast, 11.2% ± 0.1% of the K562 cells, nucleofected with the TA800G donor and TALEN αT4$_P$ plasmids, expressed GFP. Notably, compared with the 800 bp homology donor, the 200 bp homology regions resulted in a lower efficiency of targeted integration of the GFP gene (5.8% ± 2.8%) (Figure 5A). HDR-mediated targeted transgene integration at the nuclease target sites was additionally validated by bidirectional targeted integration PCR using primers binding in the GFP cassette and outside of the donor homology regions at the endogenous *TRAC* locus (Figure 5B).

After validating HDR from donor plasmids for transgene addition in K562 cells, we packaged the TA800G donor into IDLV particles and transduced CD3/CD28-activated primary T cells followed 24 hr later by αT4$_m$ nuclease electroporation. GFP expression and TCR knockout were subsequently analyzed by flow cytometry. Seven days after transduction, 64.2% ± 5% of the cells were CD3$^-$GFP$^-$, 6.9% ± 3.6% of the cells were CD3$^-$GFP$^+$, and 1.1% ± 0.5% were CD3$^+$GFP$^+$ (Figure 5C). After 2 and 3 weeks of cultivation, the frequency of GFP-expressing CD3$^-$ cells decreased to 4.5% ± 2.0% and 4.5% ± 2.1%, respectively (Figure 5C). In comparison, 3.5% ± 1.6% of IDLV control cells showed a very low GFP expression on day 7, which was reduced to 0.4% ± 0.3% and 0.4% ± 0.2% on days

15 and 21, respectively (Figure 5C). TALEN-treated cells showed a population with robust and stable expression of GFP that was absent in the IDLV control, suggesting targeted transgene incorporation (Figure 5C). PCR analysis of locus-specific integration at the 5′ and 3′ donor:endogenous locus junctions confirmed targeted integration by HDR (Figure 5D).

DISCUSSION

In this study, we demonstrate the efficient disruption of endogenous TCR expression and HDR-based targeted integration of a reporter gene mediated by TALENs and CRISPR/Cas9. In a murine model, it has been shown that inappropriate pairing of endogenous and transferred TCR chains led to GvHD following adoptive transfer of engineered T cells.[4] A number of approaches have been developed to avoid mispairing, such as ZFN-mediated knockout or RNAi-mediated knockdown of the endogenous TCR, codon optimization, or modification of the amino acid sequence for the preferential pairing of transferred TCR chains.[6,22,40–44]

For this study, we generated TALENs and CRISPR/Cas9, binding in partially overlapping regions of the *TRAC* and the *TRBC1/2* locus, and showed that TALEN activity can vary considerably with scaffold variants and the target site spacer length (Figure 2).[15,45] Notably, the 12 bp spacer architecture did not result in TALEN activity detectable by T7EI assay, likely because of the long linker connecting the TALEN DNA-binding domain and catalytic domain in the pTAL3 backbone.[26] Homodimerization of two identical TALEN monomers is of great importance regarding off-target activity because two left or two right homodimers may co-localize promiscuously and cleave unintended sequences.[28] Indeed, many reported off-target sites are cleaved by homodimers of TALENs and ZFNs.[15,17] However, specificity may come at a tradeoff for activity, as evidenced by our observation that TALENs containing the wild-type FokI domains consistently outperformed obligate heterodimeric FokI variants.

Using nuclease-expressing plasmid DNA, we achieved up to 19.9% and 12.2% knockout of TCR expression in primary T cells with CRISPR/Cas9 and TALENs, respectively. We observed DNA-dependent toxicity in primary T cells, and this can limit the effective dose able to be delivered (Figure S4).[31] In contrast, delivery of TALEN mRNA by electroporation resulted in high viability and TCR knockout efficiencies of up to 78.8% for the TCR α chain and 81.2% for the β chain on day 6 after electroporation. To our knowledge, along with the *TRAC* disruption rates shown by Poirot et al.,[46] this represents the highest TALEN-mediated TCR knockout efficiencies currently reported in the literature. This striking increase in efficiency could be because of earlier availability of higher concentrations of the nucleases delivered as mRNA and because of optimized transfection efficiency (Figure 3C; Figures S3 and S4).[21] Moreover, the use of mRNA templates abolishes the risk of genomic plasmid integration and ensures transient nuclease expression.[47]

A number of studies have reported large chromosomal deletions induced by simultaneous cleavage of two loci.[48,49] Indeed, we showed that cleavage of both *TRBC* target sites can result in a deletion of the complete sequence separating them (C1-C2 deletion) (Figure S2). We hypothesize that these chromosomal deletions resulted in a biased quantification of knockout efficiencies by deep sequencing that suggested lower knockout rates in the *TRBC1* locus as compared with the *TRBC2* locus. Due to the homology between the C1 and the C2 region, the forward primers we used for PCR amplification for T7EI assay and deep sequencing have up to two mismatches. Thus, mispriming of the C2 forward primer in the C1 region can result in the amplification of sequences with a C1-C2 deletion. In contrast, the target specificity of the C1 reverse primer prevents a successful amplification of these deletion-containing sequences (Figure S2A).

Multiple studies analyzing on- and off-target activity of different classes of designer nucleases have been published and are of great importance for translational cellular engineering.[10,16,18–20] The genome-wide IDLV capture methodology we employed is predicted to detect off-target sites with a sensitivity threshold of 1% of mutated sequences.[16,50] Using this approach, we detected a high frequency of on-target IDLV CLISs in all nuclease-treated cells, whereas none of the integration sites in IDLV-only-treated cells was located at these target sites (Table S2). Four of the six detected TALEN off-target sites were found only in samples treated with TALEN mRNA. This may be because of the differing scaffolds of TALENs delivered as plasmid DNA. However, the lower indel frequency at the respective target sites indicates lower general cleavage efficiencies for TALENs delivered as plasmid DNA. This may result in dose-dependent prevention of off-target cleavage or in cleavage activity below the detection limit of the IDLV capture assay. In accordance with this, deep sequencing of the on- and off-target sites in T cell samples resulted not only in markedly elevated target site indel frequencies, but also considerably higher off-target indel frequencies (Figure 4; Table S4). The two off-target sites that were not confirmed by deep sequencing in K562 cells (αT4 OT3 and βT4 OT3) were observed in T cells, however with very low indel frequencies (Figure 4; Table S4). Importantly, five of the six detected TALEN off-target sites were cleaved by homodimers of the respective left TALEN monomer of αT4 and βT4. Thus, usage of optimized heterodimeric versions of TALENs would prevent these off-target sites completely.

Only one off-target CLIS was found for gRNA βC1, indicating a high degree of specificity for the CRISPR/Cas9 gRNA examined in this study. In contrast, 24 off-target CLISs were detected for the control gRNA βC3. This demonstrates that currently available bioinformatics predictive tools for target sites design are able to a priori exclude target sites with the possibility of exhibiting significant off-target effects. However, although number and position of mismatches between target site and off-target site play an important role, in silico homology-based predictions can only serve as a guide for nuclease design, but do not uniformly predict bona fide off-target sites.[18,33] This is demonstrated in our observations that only 7 of the 24 experimentally determined off-target sites for βC3 were predicted by two different tools that identify off-target sites with up to four[38] or three[39] mismatches. When allowing insertions and deletions in addition to

two mismatches, the COSMID tool predicted all of the off-target sites; however, experimental validation of the 1,197 off-target sites at 823 genomic sites predicted using these parameters would be highly laborious.

We and others have previously shown that the number of off-target sites for the same type of nuclease varies greatly depending on the respective target sequence composition.[17,33,50] In our current study we observed that up to 11 mismatches were tolerated by both TALEN candidates (Figure 4; Table S3). These findings highlight the necessity of an individual and comprehensive analysis of off-target cleavage for each nuclease, particularly in the context of future translational use.

Transgenic TCR chains or chimeric antigen receptors (CARs) can be delivered efficiently to primary T cells by lentiviral or retroviral vectors that integrate at unknown positions in the genome.[1,6] As a more specific alternative, with our *TRAC*-specific GFP-expressing vector, we showed HDR-mediated targeted integration of a reporter gene into the *TRAC* locus (Figure 5C). At all analyzed time points the TALEN-treated cells comprised a population showing high GFP expression that was absent in the IDLV-only control cells (Figure 5C). The majority of these cells were $CD3^-$, indicating simultaneous TCR knockout and transgene integration into the *TRAC* target locus. The small population of $CD3^+$ and GFP^+ cells most likely represents cells with specific transgene integration into the silenced/non-productive *TRAC* allele. The donor construct is designed for subsequent transgene exchange that can be used to introduce user-defined TCR or CAR genes into the *TRAC* locus. This powerful approach supports designer cellular engineering and would allow for CD3-dependent or antigenic restimulation of the cells, if required, for expansion to therapeutic numbers.

Taken together, we report a set of TALENs and CRISPR/Cas9 reagents for specific and efficient genome editing in the constant regions of the TCR α and β chains. The demonstrated efficiency and specificity are additive to the field and further support translational application of designer nucleases for engineering T cells for adoptive cell therapy.

MATERIALS AND METHODS

TALEN and CRISPR/Cas9 gRNA Design and Generation

TALEN target sites were chosen using two versions of the online tool TAL Effector-Nucleotide Targeter (TALE-NT; https://tale-nt.cac.cornell.edu/TALENT/).[51] The old version was used for TALEN αT2-5 and βT1-5; the new version was used for αT6-9 design. TALEN assembly was accomplished by Golden Gate cloning using the Golden Gate TALEN and TAL Effector Kit 2.0.[9] Complete TALEN arrays of TALEN αT2-5 and βT1-5 were cloned into the mammalian expression vector pCMV-MCS (Agilent) after the introduction of supplementary recognition sites for AflII and XhoI. In addition, repeating the second Golden Gate reaction, αT2, αT4, βT2, and βT4 were cloned into pCAG-T7-TALEN(Sangamo)-Destination vector for homodimeric pairing and pCAG-T7-TALEN(Sangamo)-FokI-KKR-Destination or pCAG-T7-TALEN(Sangamo)-FokI-ELD-Destination vectors for heterodimeric pairing.[24] For TALEN αT6-9 the T_G backbone was used during the Golden Gate cloning procedure.[23] TALEN αT4 and βT4 were further subcloned into RCIscript-T_G backbone.[23] For in vitro transcription, the TALEN plasmids were linearized with SacI-HF and mRNA was generated using the mMESSAGE mMACHINE T3 kit (Thermo Fisher Scientific) with polyA addition using Poly(A) Tailing Kit (Thermo Fisher Scientific). The amino acid substitutions for obligate heterodimeric TALENs were introduced with the QuikChange II Site-Directed Mutagenesis kit (Agilent) and primers containing point mutations (see list of primers in the Supplemental Information). *TRAC* CRISPR/Cas9 gRNA were designed manually following the guidelines published by Cong et al.[10] For *TRBC* CRISPR/Cas9 gRNA design and in silico off-target prediction, the gRNA design tool (http://crispr.mit.edu/) was applied.[38] Chosen gRNA sequences were ordered as 5′ phosphorylated oligonucleotides and cloned into the pX330-U6-Chimeric_BB-CBh-hSpCas9 vector.[10]

Cell Culture

Cells were cultured with 5% CO_2 at 37°C. K562 and HEK293T cells were cultured in Iscove's modified Dulbecco's medium (IMDM; Gibco), supplemented with 10% fetal bovine serum (FBS) and 0.1 mg/mL penicillin and streptomycin. Peripheral blood mononuclear cells (PBMCs) were isolated from buffy coats (blood) using Ficoll density centrifugation. T cells were isolated from these using the Dynabeads Untouched Human T Cells Kit (Thermo Fisher Scientific) or the EasySep Human T Cell Isolation Kit (STEMCELL Technologies). Prior to transfection or transduction, T cells were activated for 40 hr with Dynabeads Human T-Activator CD3/CD28 (Thermo Fisher Scientific) and cultured in T cell medium (RPMI 1640 medium; Gibco), supplemented with 5% AB human serum (Thermo Fisher Scientific), 0.1 mg/mL penicillin and streptomycin, and recombinant human IL-7 and IL-15 (Miltenyi Biotec) at 5 ng/mL.

Transfection of Cells

For transfection of 293T cells, 2.5 μg of each TALEN monomer in IMDM was mixed with 18 μg PEI (Sigma-Aldrich) in IMDM, incubated at room temperature (RT) for 30 min and given to 1×10^6 cells dropwise. A total of 2×10^5 K562 cells was nucleofected in 16-well Nucleocuvette Strips with the Amaxa 4D-Nucleofector (Lonza) using the SF Cell Line 4D-Nucleofector X Kit and 1–2 μg nuclease plasmid, 4 μg TALEN mRNA, and/or 3 μg donor DNA. Delivery of TALEN plasmids (2 μg) or mRNA (2–4 μg) and CRISPR/Cas9 plasmids (1 μg) to 2–3 $\times 10^5$ T cells was done by Neon Transfection System (Thermo Fisher Scientific) in resuspension buffer T using 10 μL Neon tips and the following electroporation parameters: 1,400 V, 10 ms, 3 pulses. Transfected cells were initially plated in 96-well plates in 200 μL of antibiotic-free medium and transferred to medium containing antibiotics after 24 hr. For viability analysis, cells were counted 24 hr after electroporation using trypan blue exclusion. In the context of HDR-mediated gene transfer experiments, T cells were electroporated 24 hr after transduction or 48–72 hr after activation.

IDLV Production and Transduction of Cells

IDLV particles were produced in 293T cells using calcium phosphate transfection of a GFP transfer vector or the TA800G donor vector and

the components of a third generation lentiviral packaging system as described previously.[52] For DSB capture, K562 cells were transduced with GFP-IDLV (MOI 10) followed by nucleofection of 1×10^6 transduced cells per sample with 4–8 μg of TALEN- or CRISPR/Cas9-expressing plasmids 24 hr later. For T cell transduction 48 hr after activation or 24 hr after electroporation, 6×10^5 cells were transduced with TA800G-IDLV (MOI 50) in 200 μL of T cell medium. After 24 hr, fresh T cell medium was added and cells were cultivated at a density of 5×10^5 to 1.5×10^6 cells/mL or counted for electroporation.

T7EI Assay and On- and Off-Target Deep Sequencing

Forty-eight hours after nuclease transfection, genomic DNA was isolated and the target sites were amplified by PCR using primers for *TRAC*, *TRBC1*, or *TRBC2* included in the list of primers (see Supplemental Information). The PCR was performed with the following conditions: initial denaturation 5 min at 95°C; 30–35 cycles, denaturation at 95°C for 30 s, primer annealing at 60°C for 30 s (for variations, see list of primers in the Supplemental Information), and elongation at 72°C for 40 s; final elongation of 5 min at 72°C. 1 μL of buffer NEBuffer 2 was added to 8.5 μL of the PCR product, and the DNA was denatured and re-annealed (95°C for 5 min, 95°C to 85°C at −2°C/s, and then 85°C to 25°C at −0.1°C/s). Five units of T7EI was added for digestion of the PCR product for 15 min at 37°C. For validating deletions between the nuclease target sites in C1 and C2, PCRs were conducted with the T7EI primers and the TRBC1S_for primer included in the list of primers (see Supplemental Information). The PCRs were performed with the following parameters: initial denaturation 5 min at 94°C; 28–35 cycles, denaturation at 94°C for 30 s, primer annealing at 64°C for 30 s, and elongation at 72°C for 90 s; final elongation at 72°C for 5 min. For deep sequencing, the on- and off-target site primers were directly fused to sequencing adapters and barcodes for multiplexed Illumina MiSeq sequencing, or a two-step PCR was performed using primers containing the MiSeq adapters and barcodes (list of primers is provided in the Supplemental Information). The PCR was performed with the following conditions: initial denaturation 5 min at 95°C; 30–35 cycles, denaturation at 95°C for 30 s, primer annealing at 60°C for 30 s (for variations, see list of primers in the Supplemental Information), and elongation at 72°C for 40 s; final elongation of 5 min at 72°C. The frequency of insertions and deletions was analyzed using version 0.9.9 of the CRISPResso tool.[37] The chosen minimum average read quality was 30; only mutations occurring within a 20 bp window centered on each predicted on- or off-target site were included, and substitutions were ignored in NHEJ quantification. Reference sequences were taken from University of California, Santa Cruz (UCSC) Assembly hg19 (February 2009) (*TRBC1*/*TRBC2* sequences from hg38 [December 2013]). For NHEJ quantification, indel frequency of controls was subtracted from the respective values of treated samples.

Flow Cytometry

For flow cytometric analysis of CD3 expression, 5–6 days after transfection with nucleases, T cells were washed with staining buffer (PBS with 2% FBS) and stained for 45 min at 4°C. The allophycocyanin (APC)-eFluor 780-conjugated mouse anti-human CD3 antibody (1:100; eBioscience) or the fluorescein isothiocyanate (FITC)- or APC-conjugated mouse anti-human CD3 antibody (FITC 1:200, APC 1:50; BD Biosciences) was diluted in fluorescence-activated cell sorting (FACS) buffer. Stained cells were washed twice and resuspended in staining buffer containing 0.5 μg/mL propidium iodide (PI) for dead cell staining. For analysis of GFP expression of K562 or T cells, the cells were washed and resuspended in FACS buffer containing 0.5 μg/mL PI, and washing was repeated. Flow cytometric analyses were performed using LSRII (BD Biosciences), and data were analyzed using FlowJo software (Tree Star).

IDLV Integration Site Analysis

GFP expression of transduced cells was determined by flow cytometry after transfection with nucleases. Genomic DNA was isolated using the High Pure PCR Template Preparation Kit (Roche) after 3–4 weeks of cultivation when the frequency of GFP-expressing cells was stable. Each sample was analyzed by at least two repetitions of 3′ LAM-PCR[32] with enzymes MseI and MluCI and 3′ nrLAM-PCR[34] using 500 ng of genomic DNA each. For sequencing with the Illumina MiSeq platform, barcode-containing adapters were added to LAM-PCR products by an additional PCR step, and the integration site data were analyzed using the high-throughput insertion site analysis pipeline (HISAP).[33] Additional in silico off-target prediction for βC1 and βC3 was accomplished with the web-based COSMID tool.[39] For all analyses, the UCSC Assembly hg19 (February 2009) was used as reference genome.

Donor Construction and Targeted Integration PCR

For the 200 bp α chain donor construct (TA200G), we ordered a GeneArt Strings DNA Fragment (Thermo Fisher Scientific) containing two 200 bp regions flanking the αT4 cutting site in the *TRAC* locus and restriction sites AsiSI and SbfI for cloning into a lentiviral transfer vector in antisense direction. A GFP-expression cassette comprising a phosphoglycerate kinase (PGK) promoter and a polyA signal was cloned between the two homology sites in antisense direction using MfeI and NheI. For TA800G construction, the 200 bp homology regions were exchanged by 800 bp homology regions, amplified from Jurkat genomic DNA with primers containing AsiSI or NheI restriction sites for the 5′ homology arm and SbfI or SphI sites for the 3′ homology arm. Targeted integration PCR was performed with the following conditions: initial denaturation 5 min at 94°C; followed by 35 cycles at 94°C for 30 s, 58°C for 30 s, and 72°C for 90 s, and a final elongation of 5 min at 72°C. For 5′ targeted integration amplification, forward primers Alpha_donor200for or Alpha_donor800for and reverse primer DonorPGK were used. 3′ Targeted integration PCR was done with forward primer DonorGFPpolyA and reverse primers Alpha_donor200rev or Alpha_donor800rev (see list of primers in the Supplemental Information).

SUPPLEMENTAL INFORMATION

Supplemental Information includes five figures, five tables, and a list of primers and can be found with this article online at http://dx.doi.org/10.1016/j.omtm.2017.01.005.

AUTHOR CONTRIBUTIONS

Conceptualization, R.G., M.S., and C.v.K.; Methodology, F.K., R.G., M.S., and K.P.; Investigation, F.K.; Resources, M.J.O., J.T., and H.G.; Writing – Original Draft, F.K., R.G., M.J.O., and M.S.; Supervision, R.G., C.v.K., and M.S.

CONFLICTS OF INTEREST

The authors declare no conflict of interest.

ACKNOWLEDGMENTS

We thank Raffaele Fronza for helpful discussions. This work was supported by the European Union Seventh Framework Program (grant 601958-SUPERSIST) and NCT3.0 funding program (NCT3.0_2015.13 ImmunOmics). M.J.O. and J.T. are also thankful for the generosity of the Lindahl family, the Children's Cancer Research Fund, and the Corrigan family. M.J.O. is supported by 8UL1TR000114-02. J.T. is supported in part by R01 AR063070 and P01 CA065493. The present work was partly supported by research funds from the National Research Foundation of Korea (grant NRF-2015K1A4A3046807). Research reported in this publication was supported by the National Center for Advancing Translational Sciences of the National Institutes of Health (award UL1TR000114 to M.J.O.). The content is solely the responsibility of the authors and does not necessarily represent the official views of the National Institutes of Health.

REFERENCES

1. Morgan, R.A., Dudley, M.E., Wunderlich, J.R., Hughes, M.S., Yang, J.C., Sherry, R.M., Royal, R.E., Topalian, S.L., Kammula, U.S., Restifo, N.P., et al. (2006). Cancer regression in patients after transfer of genetically engineered lymphocytes. Science *314*, 126–129.
2. Johnson, L.A., Morgan, R.A., Dudley, M.E., Cassard, L., Yang, J.C., Hughes, M.S., Kammula, U.S., Royal, R.E., Sherry, R.M., Wunderlich, J.R., et al. (2009). Gene therapy with human and mouse T-cell receptors mediates cancer regression and targets normal tissues expressing cognate antigen. Blood *114*, 535–546.
3. Heemskerk, M.H., Hagedoorn, R.S., van der Hoorn, M.A., van der Veken, L.T., Hoogeboom, M., Kester, M.G., Willemze, R., and Falkenburg, J.H. (2007). Efficiency of T-cell receptor expression in dual-specific T cells is controlled by the intrinsic qualities of the TCR chains within the TCR-CD3 complex. Blood *109*, 235–243.
4. Bendle, G.M., Linnemann, C., Hooijkaas, A.I., Bies, L., de Witte, M.A., Jorritsma, A., Kaiser, A.D., Pouw, N., Debets, R., Kieback, E., et al. (2010). Lethal graft-versus-host disease in mouse models of T cell receptor gene therapy. Nat. Med *16*, 565–570, 1p following 570.
5. van Loenen, M.M., de Boer, R., Amir, A.L., Hagedoorn, R.S., Volbeda, G.L., Willemze, R., van Rood, J.J., Falkenburg, J.H., and Heemskerk, M.H. (2010). Mixed T cell receptor dimers harbor potentially harmful neoreactivity. Proc. Natl. Acad. Sci. USA *107*, 10972–10977.
6. Provasi, E., Genovese, P., Lombardo, A., Magnani, Z., Liu, P.Q., Reik, A., Chu, V., Paschon, D.E., Zhang, L., Kuball, J., et al. (2012). Editing T cell specificity towards leukemia by zinc finger nucleases and lentiviral gene transfer. Nat. Med. *18*, 807–815.
7. Miller, J.C., Tan, S., Qiao, G., Barlow, K.A., Wang, J., Xia, D.F., Meng, X., Paschon, D.E., Leung, E., Hinkley, S.J., et al. (2011). A TALE nuclease architecture for efficient genome editing. Nat. Biotechnol. *29*, 143–148.
8. Rouet, P., Smih, F., and Jasin, M. (1994). Introduction of double-strand breaks into the genome of mouse cells by expression of a rare-cutting endonuclease. Mol. Cell. Biol. *14*, 8096–8106.
9. Cermak, T., Doyle, E.L., Christian, M., Wang, L., Zhang, Y., Schmidt, C., Baller, J.A., Somia, N.V., Bogdanove, A.J., and Voytas, D.F. (2011). Efficient design and assembly of custom TALEN and other TAL effector-based constructs for DNA targeting. Nucleic Acids Res. *39*, e82.
10. Cong, L., Ran, F.A., Cox, D., Lin, S., Barretto, R., Habib, N., Hsu, P.D., Wu, X., Jiang, W., Marraffini, L.A., and Zhang, F. (2013). Multiplex genome engineering using CRISPR/Cas systems. Science *339*, 819–823.
11. Mali, P., Yang, L., Esvelt, K.M., Aach, J., Guell, M., DiCarlo, J.E., Norville, J.E., and Church, G.M. (2013). RNA-guided human genome engineering via Cas9. Science *339*, 823–826.
12. Fine, E.J., Cradick, T.J., Zhao, C.L., Lin, Y., and Bao, G. (2014). An online bioinformatics tool predicts zinc finger and TALE nuclease off-target cleavage. Nucleic Acids Res. *42*, e42.
13. Pattanayak, V., Ramirez, C.L., Joung, J.K., and Liu, D.R. (2011). Revealing off-target cleavage specificities of zinc-finger nucleases by in vitro selection. Nat. Methods *8*, 765–770.
14. Fu, Y., Foden, J.A., Khayter, C., Maeder, M.L., Reyon, D., Joung, J.K., and Sander, J.D. (2013). High-frequency off-target mutagenesis induced by CRISPR-Cas nucleases in human cells. Nat. Biotechnol. *31*, 822–826.
15. Gabriel, R., Lombardo, A., Arens, A., Miller, J.C., Genovese, P., Kaeppel, C., Nowrouzi, A., Bartholomae, C.C., Wang, J., Friedman, G., et al. (2011). An unbiased genome-wide analysis of zinc-finger nuclease specificity. Nat. Biotechnol. *29*, 816–823.
16. Wang, X., Wang, Y., Wu, X., Wang, J., Wang, Y., Qiu, Z., Chang, T., Huang, H., Lin, R.J., and Yee, J.K. (2015). Unbiased detection of off-target cleavage by CRISPR-Cas9 and TALENs using integrase-defective lentiviral vectors. Nat. Biotechnol. *33*, 175–178.
17. Osborn, M.J., Starker, C.G., McElroy, A.N., Webber, B.R., Riddle, M.J., Xia, L., DeFeo, A.P., Gabriel, R., Schmidt, M., von Kalle, C., et al. (2013). TALEN-based gene correction for epidermolysis bullosa. Mol. Ther. *21*, 1151–1159.
18. Tsai, S.Q., Zheng, Z., Nguyen, N.T., Liebers, M., Topkar, V.V., Thapar, V., Wyvekens, N., Khayter, C., Iafrate, A.J., Le, L.P., et al. (2015). GUIDE-seq enables genome-wide profiling of off-target cleavage by CRISPR-Cas nucleases. Nat. Biotechnol. *33*, 187–197.
19. Frock, R.L., Hu, J., Meyers, R.M., Ho, Y.J., Kii, E., and Alt, F.W. (2015). Genome-wide detection of DNA double-stranded breaks induced by engineered nucleases. Nat. Biotechnol. *33*, 179–186.
20. Osborn, M.J., Webber, B.R., Knipping, F., Lonetree, C.L., Tennis, N., DeFeo, A.P., McElroy, A.N., Starker, C.G., Lee, C., Merkel, S., et al. (2016). Evaluation of TCR gene editing achieved by TALENs, CRISPR/Cas9, and megaTAL nucleases. Mol. Ther. *24*, 570–581.
21. Berdien, B., Mock, U., Atanackovic, D., and Fehse, B. (2014). TALEN-mediated editing of endogenous T-cell receptors facilitates efficient reprogramming of T lymphocytes by lentiviral gene transfer. Gene Ther. *21*, 539–548.
22. Bunse, M., Bendle, G.M., Linnemann, C., Bies, L., Schulz, S., Schumacher, T.N., and Uckert, W. (2014). RNAi-mediated TCR knockdown prevents autoimmunity in mice caused by mixed TCR dimers following TCR gene transfer. Mol. Ther. *22*, 1983–1991.
23. Carlson, D.F., Tan, W., Lillico, S.G., Stverakova, D., Proudfoot, C., Christian, M., Voytas, D.F., Long, C.R., Whitelaw, C.B., and Fahrenkrug, S.C. (2012). Efficient TALEN-mediated gene knockout in livestock. Proc. Natl. Acad. Sci. USA *109*, 17382–17387.
24. Hermann, M., Cermak, T., Voytas, D.F., and Pelczar, P. (2014). Mouse genome engineering using designer nucleases. J. Vis. Exp. (86), e50930.
25. Christian, M., Cermak, T., Doyle, E.L., Schmidt, C., Zhang, F., Hummel, A., Bogdanove, A.J., and Voytas, D.F. (2010). Targeting DNA double-strand breaks with TAL effector nucleases. Genetics *186*, 757–761.
26. Mussolino, C., Morbitzer, R., Lütge, F., Dannemann, N., Lahaye, T., and Cathomen, T. (2011). A novel TALE nuclease scaffold enables high genome editing activity in combination with low toxicity. Nucleic Acids Res. *39*, 9283–9293.
27. Bedell, V.M., Wang, Y., Campbell, J.M., Poshusta, T.L., Starker, C.G., Krug, R.G., 2nd, Tan, W., Penheiter, S.G., Ma, A.C., Leung, A.Y., et al. (2012). In vivo genome editing using a high-efficiency TALEN system. Nature *491*, 114–118.
28. Miller, J.C., Holmes, M.C., Wang, J., Guschin, D.Y., Lee, Y.L., Rupniewski, I., Beausejour, C.M., Waite, A.J., Wang, N.S., Kim, K.A., et al. (2007). An improved

zinc-finger nuclease architecture for highly specific genome editing. Nat. Biotechnol. *25*, 778–785.

29. Cade, L., Reyon, D., Hwang, W.Y., Tsai, S.Q., Patel, S., Khayter, C., Joung, J.K., Sander, J.D., Peterson, R.T., and Yeh, J.R. (2012). Highly efficient generation of heritable zebrafish gene mutations using homo- and heterodimeric TALENs. Nucleic Acids Res. *40*, 8001–8010.
30. Nakajima, K., and Yaoita, Y. (2013). Comparison of TALEN scaffolds in Xenopus tropicalis. Biol. Open *2*, 1364–1370.
31. Zhao, Y., Zheng, Z., Cohen, C.J., Gattinoni, L., Palmer, D.C., Restifo, N.P., Rosenberg, S.A., and Morgan, R.A. (2006). High-efficiency transfection of primary human and mouse T lymphocytes using RNA electroporation. Mol. Ther. *13*, 151–159.
32. Schmidt, M., Schwarzwaelder, K., Bartholomae, C., Zaoui, K., Ball, C., Pilz, I., Braun, S., Glimm, H., and von Kalle, C. (2007). High-resolution insertion-site analysis by linear amplification-mediated PCR (LAM-PCR). Nat. Methods *4*, 1051–1057.
33. Arens, A., Appelt, J.U., Bartholomae, C.C., Gabriel, R., Paruzynski, A., Gustafson, D., Cartier, N., Aubourg, P., Deichmann, A., Glimm, H., et al. (2012). Bioinformatic clonality analysis of next-generation sequencing-derived viral vector integration sites. Hum. Gene Ther. Methods *23*, 111–118.
34. Paruzynski, A., Arens, A., Gabriel, R., Bartholomae, C.C., Scholz, S., Wang, W., Wolf, S., Glimm, H., Schmidt, M., and von Kalle, C. (2010). Genome-wide high-throughput integrome analyses by nrLAM-PCR and next-generation sequencing. Nat. Protoc. *5*, 1379–1395.
35. Gabriel, R., Eckenberg, R., Paruzynski, A., Bartholomae, C.C., Nowrouzi, A., Arens, A., Howe, S.J., Recchia, A., Cattoglio, C., Wang, W., et al. (2009). Comprehensive genomic access to vector integration in clinical gene therapy. Nat. Med. *15*, 1431–1436.
36. Dsouza, M., Larsen, N., and Overbeek, R. (1997). Searching for patterns in genomic data. Trends Genet. *13*, 497–498.
37. Pinello, L., Canver, M.C., Hoban, M.D., Orkin, S.H., Kohn, D.B., Bauer, D.E., and Yuan, G.C. (2016). Analyzing CRISPR genome-editing experiments with CRISPResso. Nat. Biotechnol. *34*, 695–697.
38. Hsu, P.D., Scott, D.A., Weinstein, J.A., Ran, F.A., Konermann, S., Agarwala, V., Li, Y., Fine, E.J., Wu, X., Shalem, O., et al. (2013). DNA targeting specificity of RNA-guided Cas9 nucleases. Nat. Biotechnol. *31*, 827–832.
39. Cradick, T.J., Qiu, P., Lee, C.M., Fine, E.J., and Bao, G. (2014). COSMID: a web-based tool for identifying and validating CRISPR/Cas off-target sites. Mol. Ther. Nucleic Acids *3*, e214.
40. Sommermeyer, D., and Uckert, W. (2010). Minimal amino acid exchange in human TCR constant regions fosters improved function of TCR gene-modified T cells. J. Immunol. *184*, 6223–6231.
41. Bialer, G., Horovitz-Fried, M., Ya'acobi, S., Morgan, R.A., and Cohen, C.J. (2010). Selected murine residues endow human TCR with enhanced tumor recognition. J. Immunol. *184*, 6232–6241.
42. Scholten, K.B., Kramer, D., Kueter, E.W., Graf, M., Schoedl, T., Meijer, C.J., Schreurs, M.W., and Hooijberg, E. (2006). Codon modification of T cell receptors allows enhanced functional expression in transgenic human T cells. Clin. Immunol. *119*, 135–145.
43. Kuball, J., Dossett, M.L., Wolfl, M., Ho, W.Y., Voss, R.H., Fowler, C., and Greenberg, P.D. (2007). Facilitating matched pairing and expression of TCR chains introduced into human T cells. Blood *109*, 2331–2338.
44. Cohen, C.J., Li, Y.F., El-Gamil, M., Robbins, P.F., Rosenberg, S.A., and Morgan, R.A. (2007). Enhanced antitumor activity of T cells engineered to express T-cell receptors with a second disulfide bond. Cancer Res. *67*, 3898–3903.
45. Christian, M.L., Demorest, Z.L., Starker, C.G., Osborn, M.J., Nyquist, M.D., Zhang, Y., Carlson, D.F., Bradley, P., Bogdanove, A.J., and Voytas, D.F. (2012). Targeting G with TAL effectors: a comparison of activities of TALENs constructed with NN and NK repeat variable di-residues. PLoS ONE *7*, e45383.
46. Poirot, L., Philip, B., Schiffer-Mannioui, C., Le Clerre, D., Chion-Sotinel, I., Derniame, S., Potrel, P., Bas, C., Lemaire, L., Galetto, R., et al. (2015). Multiplex genome-edited T-cell manufacturing platform for "off-the-shelf" adoptive T-cell Immunotherapies. Cancer Res. *75*, 3853–3864.
47. Wang, Z., Troilo, P.J., Wang, X., Griffiths, T.G., Pacchione, S.J., Barnum, A.B., Harper, L.B., Pauley, C.J., Niu, Z., Denisova, L., et al. (2004). Detection of integration of plasmid DNA into host genomic DNA following intramuscular injection and electroporation. Gene Ther. *11*, 711–721.
48. Mussolino, C., Alzubi, J., Fine, E.J., Morbitzer, R., Cradick, T.J., Lahaye, T., Bao, G., and Cathomen, T. (2014). TALENs facilitate targeted genome editing in human cells with high specificity and low cytotoxicity. Nucleic Acids Res. *42*, 6762–6773.
49. Young, C.S., Hicks, M.R., Ermolova, N.V., Nakano, H., Jan, M., Younesi, S., Karumbayaram, S., Kumagai-Cresse, C., Wang, D., Zack, J.A., et al. (2016). A single CRISPR-Cas9 deletion strategy that targets the majority of DMD patients restores dystrophin function in hiPSC-derived muscle cells. Cell Stem Cell *18*, 533–540.
50. Gabriel, R., von Kalle, C., and Schmidt, M. (2015). Mapping the precision of genome editing. Nat. Biotechnol. *33*, 150–152.
51. Doyle, E.L., Booher, N.J., Standage, D.S., Voytas, D.F., Brendel, V.P., Vandyk, J.K., and Bogdanove, A.J. (2012). TAL effector-nucleotide targeter (TALE-NT) 2.0: tools for TAL effector design and target prediction. Nucleic Acids Res. *40*, W117–W122.
52. Lombardo, A., Genovese, P., Beausejour, C.M., Colleoni, S., Lee, Y.L., Kim, K.A., Ando, D., Urnov, F.D., Galli, C., Gregory, P.D., et al. (2007). Gene editing in human stem cells using zinc finger nucleases and integrase-defective lentiviral vector delivery. Nat. Biotechnol. *25*, 1298–1306.
53. Giudicelli, V., Chaume, D., and Lefranc, M.P. (2005). IMGT/GENE-DB: a comprehensive database for human and mouse immunoglobulin and T cell receptor genes. Nucleic Acids Res. *33*, D256–D261.